Differential Modulation of Binding Loop Flexibility and Stability by Arg^{50} and Arg^{52} in *Cucurbita maxima* Trypsin Inhibitor-V Deduced by Trypsin-Catalyzed Hydrolysis and NMR Spectroscopy†

Mengli Cai,‡ Ying Huang,‡ Om Prakash,‡ Lisa Wen,§ Steven P. Dunkelbarger,§ Jeng-Kuen Huang,§ Jianhua Liu,‡ and Ramaswamy Krishnamoorthi*,‡

Department of Biochemistry, Kansas State University, Manhattan, Kansas 66506, and Department of Chemistry, Western Illinois University, Macomb, Illinois 61455

Received December 21, 1995; Revised Manuscript Received February 15, 1996⊗

ABSTRACT: The side chains of Arg^{50} and Arg^{52} in *Cucurbita maxima* trypsin inhibitor-V (CMTI-V) anchor the binding loop to the scaffold region [Cai, M., Gong, Y., Kao, J. L.-F., & Krishnamoorthi, R. (1995) *Biochemistry 34*, 5201−5211]. The consequences of these hydrogen-bonding and electrostatic interactions on the conformational flexibility and stability of the binding loop were evaluated by trypsin-catalyzed hydrolysis of CMTI-V mutants, in which each of the two arginines was individually replaced with Ala, Lys, or Gln by genetic engineering methods. All the mutants exhibited significantly increased vulnerability to the protease attack at many sites, including the reactive-site (Lys^{44}-Asp^{45} peptide bond), with the R50 mutants showing much more pronounced effects than the R52 counterparts. For CMTI-V and the mutants studied, a qualitative correlation was inferred between binding loop flexibility and retention time on a reverse-phase high-pressure liquid chromatography C-18 column. The R50 mutants were found to be more flexible than the corresponding R52 versions. These results demonstrate that Arg^{50} contributes more to the stability and function of CMTI-V. The differing strengths of the hydrogen bonds made by Arg^{50} and Arg^{52} were characterized by determining the internal dynamics of their side chains at pH 5.0 and 2.5: ^{15}N NMR longitudinal and transverse relaxation rates and $^{15}N-^{1}H$ nuclear Overhauser effect (NOE) enhancements were measured for the main-chain and side-chain NH groups in ^{15}N-labeled recombinant CMTI-V (rCMTI-V) and the model-free parameters [Lipari, G., & Szabo, A. (1982) *J. Am. Chem. Soc. 104*, 4546−4559; 4559−4570] were calculated. At both pH 5.0 and 2.5, the arginines at positions 26, 47, 58, and 66 are found to be highly mobile, as the calculated general order parameters, S^2 values, of their $N_\epsilon H$ groups fall in the range 0.03−0.18. The corresponding values for Arg^{50} and Arg^{52} are 0.73 and 0.63, respectively, at pH 5.0, thus confirming that the two arginines are rigid and hydrogen-bonded. At pH 2.5, these hydrogen bonds are still retained with Arg^{50} appearing to be more restrained ($S^2 = 0.71$) than Arg^{52} ($S^2 = 0.56$). This is consistent with a greater contribution by Arg^{50} to the conformational stability of the reactive-site loop in CMTI-V. The results also indicate that the Arg^{50} and Arg^{52} side chains are not hydrogen-bonded to carboxylate groups, which would be protonated at pH 2.5 and, hence, unavailable for hydrogen-bonding interactions. The overall folding of rCMTI-V appears not to be significantly affected by the pH change, as indicated by comparisons of ^{1}H and ^{15}N chemical shifts, sequential NOE cross-peaks, and S^2 values of the backbone atoms, and the conserved side-chain dynamics of Trp^{9} and Trp^{54}—residues that are involved in hydrophobic and hydrogen-bonding interactions with others in the protein core and the binding loop, respectively.

Protein inhibitors of serine proteases act on their cognate enzymes according to the standard mechanism (Laskowski & Kato, 1980) which is described as follows:

$$I + E \rightleftarrows I{\cdot}E \rightleftarrows I^* + E$$

where I and I* are the intact and reactive-site hydrolyzed or modified inhibitor, respectively, and E is the enzyme. Thus, it is seen that there is an equilibrium between both forms of the inhibitor, which is defined by the hydrolysis constant

$$K_{hyd} = [I^*]/[I] \quad (1)$$

The K_{hyd} value is a measure of the standard free-energy difference ($\Delta G°$) between the two forms. Therefore, one way of assessing the effect of a single amino acid substitution on side-chain−side-chain interactions in a serine proteinase inhibitor is to measure the K_{hyd} value of the mutant. Standard enthalpy ($\Delta H°$) and entropy ($\Delta S°$) contributions to the equilibrium can be evaluated from the temperature dependence of $\Delta G°$, which give further insight into structural differences between the intact and clipped inhibitor. Ardelt and Laskowski (1991) have determined K_{hyd} values in the range 0.4 to ∼35 for a set of 42 variants of ovomucoid third domain, a serine proteinase inhibitor of 56 residues.

† This work has been supported by grants from the National Institutes of Health (HL-40789 to R.K. and HL-52235 to L.W.) and the American Heart Association, Kansas Affiliate (KS-95-GS-14 to R.K.). R.K. is supported by an NIH Research Career Development Award (HL-03131). The 11.75 tesla NMR instrument at KSU was purchased with funds from an NSF-EPSCoR grant. This is contribution 96-363-J from the Kansas Agricultural Experiment Station.

* To whom correspondence should be addressed. Phone: (913) 532-6262. FAX: (913) 532-7278. E-mail: krish@ksu.ksu.edu.

‡ Department of Biochemistry, Kansas State University, Manhattan, KS 66506.

§ Department of Chemistry, Western Illinois University, Macomb, IL 61455.

⊗ Abstract published in *Advance ACS Abstracts,* April 1, 1996.

0006-2960/96/0435-4784$12.00/0

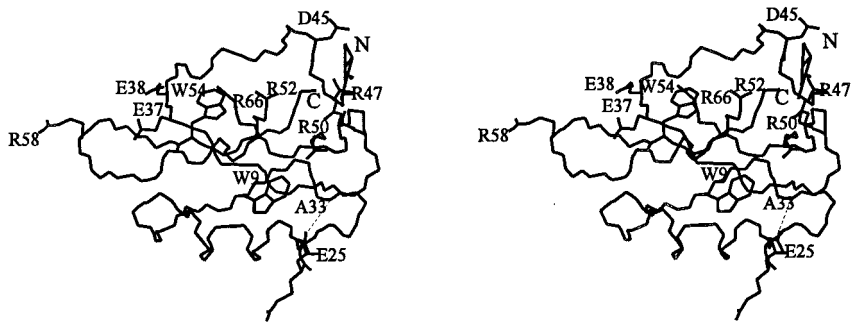

FIGURE 1: Stereoview of the refined average solution structure of rCMTI-V (Liu et al., 1996) depicting the side-chains of six arginines, three glutamates, two tryptophans, and one aspartate present in the molecule. The proposed hydrogen bond between N*H* of Ala^{33} and the side-chain oxygen of Glu^{25} is indicated by the dotted line. Only the main-chain atoms (N, C_α, and $C_{C=O}$) of other residues are shown.

Cucurbita maxima trypsin inhibitor-V (CMTI-V,[1] ~7 kDa) of the potato inhibitor I family is a specific inhibitor of human blood coagulation factor XIIa; its reactive-site is the Lys^{44}-Asp^{45} (P_1-P_1') peptide bond (Krishnamoorthi et al., 1990). We recently reported the three-dimensional solution structures of intact and modified CMTI-V (Cai et al., 1995a,b) and utilized structural knowledge to explain the functional and thermodynamic differences between the two forms. In addition, the solution structure and backbone dynamics of recombinant CMTI-V (rCMTI-V) have also been characterized (Liu et al., 1996), which shows that the less-ordered binding loop in the inhibitor indeed exhibits greater flexibility, compared to the rest of the molecule. CMTI-V is the first disulfide-containing member of the potato I family, whose three-dimensional structure has been determined to date. Both solid and solution phase three-dimensional structures are available for two other members of the potato I family: chymotrypsin inhibitor 2 (CI-2; McPhalen & James, 1987; Clore et al., 1987a,b) and eglin c (Hipler et al., 1992; Hyberts et al., 1992).

An interesting structural aspect of CMTI-V is the existence of interactions between the binding loop and the protein core that are mediated by the hydrogen-bonding Arg^{50} and Arg^{52} side chains (Figure 1; Liu et al., 1996). Our structural studies so far (Cai et al., 1995a,b; Liu et al., 1996) have provided evidence in the form of homo- and heteronuclear coupling constants (Cai et al., 1995c−e), for the rigid conformation of Arg^{52} and a hydrogen-bonding interaction has been proposed between the side chain of Arg^{52} and the side-chain oxygen of Thr^{43}. In the case of Arg^{50}, because of the chemical shift degeneracy of its δ-methylene hydrogens, its rigidity, and hence its hydrogen-bondedness, was inferred from the χ^1 torsion angle determination and hydrogen-exchange studies (Cai et al., 1995a). Of the several possibilities that included both side-chain and main-chain oxygen atoms, the side-chain oxygen of Asp^{45} was picked to be the most likely hydrogen-bonding partner. Variants of rCMTI-V, in which Arg^{50} and Arg^{52} have been individually substituted by other amino acids, are found to be poor inhibitors of factor XIIa (Wen et al., unpublished results). The hydrolyzed form of the native protein (CMTI-V*) shows a significantly reduced inhibitory activity toward both trypsin and factor XIIa, and this has been attributed to the increased flexibility of the cleaved binding loop (Cai et al., 1995b). The anchoring interactions provided by both Arg^{50} and Arg^{52} are found to be retained in the solution structure of CMTI-V* (Cai et al., 1995b).

Herein we demonstrate the contribution of Arg^{50} and Arg^{52} to the conformational flexibility and stability of the binding loop, and hence the whole protein molecule, by characterizing the susceptibility of rCMTI-V mutants to proteolysis by trypsin. For the mutants studied, the flexibility of the binding loop appears to influence the inhibitor's retention time on a reverse-phase high-pressure liquid chromatography (RP-HPLC) column. We also present NMR determination of the side-chain dynamics of Arg^{50} and Arg^{52} at two different acidic pHs as a structural probe and characterize the difference in strength between the hydrogen bonds made by these two residues. In earlier other studies, NMR relaxation measurements have been utilized to obtain information on protein dynamics (Peng & Wagner, 1994). Recently, Buck et al. (1995) have determined the side-chain dynamics of arginines and glutamines in lysozyme and identified structural factors that contribute to their mobility. Shaw et al. (1995) have compared the backbone dynamics of CI-2 and the copmlex formed between two fragments of CI-2 and drawn inferences regarding the mechanism of inhibition.

MATERIALS AND METHODS

Proteins. Trypsin inhibitors from pumpkin (*C. maxima*) seeds were isolated and purified as described previously (Krishnamoorthi et al., 1990). CMTI-III (M_r ~ 3 kDa), a squash family member (Wieczorek et al., 1985), and CMTI-V were used in the present study. rCMTI-V and mutants were expressed in *Escherichia coli* and purified using a modification of the reported procedure (Wen et al., 1993): the pH of the cell-free extract was adjusted to 2.0, and precipitated impurities were removed by centrifugation. rCTMI-V or the mutant was salted out from the supernatant with 90% ammonium sulfate. Final purification was achieved by means of RP-HPLC. Pure reactive-site hydrolyzed inhibitors were prepared as described by Cai et al. (1995b).

Uniformly ^{15}N-labeled rCMTI-V needed for NMR studies was prepared in a similar manner from *E. coli* cells grown in a medium containing $^{15}NH_4Cl$ as the sole nitrogen source. The recombinant protein used in the present study had an extra N-terminal glycine residue and was, unlike the native

[1] Abbreviations: CMTI, *C. maxima* trypsin inhibitor; rCMTI-V, recombinant *C. maxima* trypsin inhibitor-V; CMTI-V*, reactive-site hydrolyzed *C. maxima* trypsin inhibitor-V; RP-HPLC, reverse-phase high-pressure liquid chromatography; NMR, nuclear magnetic resonance; NOE, nuclear Overhauser effect; HSQC, heteronuclear single-quantum coherence; HMQC, heteronuclear multiple-quantum coherence; TOCSY, total correlated spectroscopy; NOESY, nuclear Overhauser effect spectroscopy; CPMG, Carr−Purcell−Meiboom−Gill; SD, standard deviation; ppm, parts per million; CI-2. chymotrypsin inhibitor-2 from barley seeds.

protein, unacetylated (Huang et al., unpublished results). A 5 mM sample of the labeled protein was prepared in 90% H_2O/10% D_2O (v/v) that contained 50 mM KCl at pH 5.0. After NMR data collection, the pH of the same sample was lowered to 2.5 and comparative NMR measurements were carried out. rCMTI-V was found to undergo slow conformational changes at pH 2.0, as indicated by shifted cross-peaks in NMR spectra. At pH 2.5, the protein was found to be stable over a period of 2 months, as indicated by unchanged chemical shifts of cross-peaks and non-appearance of any new cross-peaks. Therefore, pH 2.5 was chosen for the present comparative study.

Determination of Hydrolysis Constant, K_{hyd}. The K_{hyd} value was determined by measuring the ratio of areas of RP-HPLC peaks corresponding to the hydrolyzed and intact inhibitors in the equilibrium mixture. The equilibrium at 23 °C was reached by incubating either the intact or the hydrolyzed inhibitor with 5% (by mole) trypsin in 50 mM potassium phosphate buffer at pH 6.75 over a period of time and monitoring the progress of the reaction by RP-HPLC until no change was noticed in the relative areas of the HPLC peaks; at other temperatures, the equilibrium mixture was obtained by incubating the intact protein with 5 mole% trypsin. Peak area integration was carried out using a Varian HPLC software (Star Chromatography Workstation). Thermodynamic quantities, $\Delta S°$ and $\Delta H°$, were estimated from the temperature dependence of K_{hyd} in the range 4−30 °C. Because of the rapid breakdown brought about by trypsin, K_{hyd} values and other thermodynamic quantities were not determined for the five mutants used in this study.

RP-HPLC Retention Times. Retention times of rCMTI-V and the mutants used in this study were determined with a Varian HPLC instrument (model 2510) fitted with a Varian C-18 column; two solvents, 0.1 % (v/v) trifluoroacetic acid in water (solvent A) and 0.1% (v/v) trifluoroacetic acid in acetonitrile (solvent B), were used for the eluent mixture. For all the experiments, the same batch of eluents was utilized. In the case of intact and reactive-site hydrolyzed CMTI-III, CMTI-V, and rCMTI-V, composition of the eluent was changed by increasing the amount of solvent B in the mixture from its initial value of 10% at the rate of 0.5% per min for a period of 60 min. The flow rate was maintained at 2 mL/min. In the case of rCMTI-V and all the five mutants, solvent B in the elution mixture was increased 1% every 4 min for a period of 40 min, starting from its initial value of 36%. In these experiments, the observed RP-HPLC retention time was thus a measure of the hydrophobicity of the protein molecule eluted, as the hydrophobicity of the eluent increased with increasing amount of solvent B in the mixture.

NMR Spectroscopy. All NMR experiments were performed at 30 °C on a 11.75 T (500 MHZ for ^1H) Varian UNITY *plus* instrument. Data processing and analysis were done using the Varian VNMR software (version 4.3B) on a Silicon Graphics Indigo^2 XZ workstation. TOCSY (Bax & Davis, 1985), ^{15}N-edited HSQC-TOCSY (Bodenhausen & Ruben, 1980; Cavannagh et al., 1991; Palmer et al., 1991), NOESY (Anil Kumar, et al., 1980), and ^{15}N-edited HMQC-NOESY (Müller, 1979; Bax et al., 1983) experiments were each carried out with a spectral width of 7000 Hz over 2K data points; 256 increments were used. The data matrix was zero-filled to 4K × 4K and processed. The reported ^1H chemical shifts were relative to a value of 4.71 ppm assigned to the H_2O peak at 30 °C. The ^{15}N chemical shifts were determined relative to CH_3NO_2 with an assigned ^{15}N chemical shift of 380.23 ppm from liquid NH_3 (Live et al., 1984).

^{15}N Relaxation Measurements and Analysis. Spin−lattice and spin−spin relaxation rate constants (R_1 and R_2, respectively) and $^1H-^{15}N$ steady state NOEs were measured using inversion−recovery (Vold et al., 1968), Carr−Purcell−Meiboom−Gill (CPMG; Meiboom & Gill, 1958), and steady state NOE (Noggle & Shirmer, 1971) experiments, respectively; sensitivity-enhanced proton-detected $^1H-^{15}N$ heteronuclear 2D pulse sequences (Kördel et al., 1992; Skelton et al., 1993) were used. For all the three kinds of experiments, 192 increments of 4K data points were collected. Recycling delays of 3 s for R_1 and R_2 experiments and 5 s for NOE experiments were used. Spectral widths were set to 3850 Hz for the ^1H-dimension and 3500 Hz for the ^{15}N-dimension. For R_1 determination, eight experiments with relaxation delays of 0.008, 0.050, 0.120, 0.250, 0.400, 0.700, 1.100, and 2.500 s were performed; for R_2 determination, seven delays of 0.014, 0.030, 0.060, 0.150, 0.250, 0.400, and 0.700 s were used. In the earlier work (Liu et al., 1996), relaxation and NOE experiments were performed with a shorter recycling delay of 2 s, and hence relaxation parameters could not be reliably determined for side-chain $^{15}N-^1H$ groups. Furthermore, for the present comparative study of rCMTI-V at two different pHs, it was considered important to collect data under identical instrumental conditions.

Relaxation rate constants and NOE enhancements were calculated from cross-peak heights in the $^1H-^{15}N$ correlation spectra. The longitudinal relaxation rate constant, R_1, was obtained by a three-parameter nonlinear least-squares fit of the equation

$$I(t) = I_\infty - [I_\infty - I_0]\exp(-R_1 t) \quad (2)$$

where I_0 and I_∞ are adjustable parameters representing the initial and final cross-peak heights, respectively. The transverse relaxation rate constant, R_2, was obtained through a two-parameter nonlinear least-squares fit of the equation

$$I(t) = I_0 \exp(-R_2 t) \quad (3)$$

or a three-parameter nonlinear least-squares fit of the equation

$$I(t) = I_0 \exp(-R_2 t) + I_\infty \quad (4)$$

The uncertainties of R_1 and R_2 were obtained from the standard deviations of the curve fits. NOEs were calculated from the ratio of cross-peak heights with and without proton saturation during the 5 s recycling delay. Three sets of NOE experiments with and without proton saturation were recorded for both pH 5.0 and 2.5 samples. In each case, nine NOE values were calculated by dividing cross-peak heights in each experiment with proton saturation by cross-peak heights from all three experiments without proton saturation. The average of the nine NOE values was used for model-free calculations; uncertainties were calculated from the standard deviation of nine individual NOE values.

The ^{15}N relaxation data thus obtained were analyzed using the model-free formalism of Lipari and Szabo (1982a,b), with the extension of Clore et al. (1990). Calculations were performed using the software, model-free (version 3.0), provided by Dr. Arthur G. Palmer, III, Columbia University,

New York. An average R_2/R_1 ratio was first calculated of all the main-chain and side-chain NH groups, and the ones with less than one standard deviation (SD) from the average value was selected to estimate and optimize the overall tumbling time, τ_m (Clore et al., 1990). General order parameters, S^2, effective internal correlation times, τ_e, and the chemical exchange term, Δ_{ex}, were calculated simultaneously for all NHs at the fixed τ_m optimized from pH 5.0 and 2.5 data sets, using standard methods (Clore et al., 1990; Palmer et al., 1991; Stone et al., 1992; Shaw et al., 1995).

RESULTS AND DISCUSSION

Trypsin-Catalyzed Hydrolysis of rCMTI-V and Mutants. RP-HPLC results of a mixture of rCMTI-V and 5 mole% trypsin at room temperature (23 °C) are shown at three different time intervals in Figure 2 (panel A). The equilibrium of hydrolysis ($K_{hyd} \approx 7$) was found to be reached within 2 days (middle trace). Determination of its temperature dependence (Figure 1 in supporting information) yields the following estimates: $\Delta H° \approx 2$ Kcal/mol; $\Delta S° \approx 11$ eu, values similar to those obtained in the case of the native protein (Cai et al., 1995b). However, after 9 days (Figure 2A; bottom trace), rCMTI-V* was found to be fragmented by the protease, as evidenced by the appearance of new peaks at the expense of the rCMTI-V* peak. Results obtained with the mutants, R52K-rCMTI-V and R50K-rCMTI-V, are shown in panels B and C, respectively, of Figure 2. In the case of R50K-rCMTI-V, 2 mole% trypsin was used. It is seen that these mutants are rapidly hydrolyzed by trypsin into smaller fragments, as compared to rCMTI-V. Of the two mutants, R50K-rCMTI-V is found to be much more vulnerable to hydrolysis. Similar observations were made with the other mutants (not shown)—R52A, R50A, and R50Q. While R52A-rCMTI-V underwent proteolysis within 3 days, R50A- and R50Q-rCMTI-V were fragmented within 1 h after incubation with 5 mole% trypsin. These results indicate that the two anchors to the binding loop, Arg[50] and Arg[52], confer stability on the inhibitor against proteolysis by trypsin. They also assign a dominant role to Arg[50]. Recent work with the Arg mutants of rCMTI-V has shown that inhibition of factor XIIa is drastically reduced by the Arg→Ala substitution (Wen et al., unpublished results). Because binding affinity and stability against protease attack are most likely related to protein flexibility, in particular, that of the binding loop, the conclusion that the side chains of Arg[50] and Arg[52] are involved in strong hydrogen-bonding interactions with the reactive-site loop (Figure 1) in solution is fortified.

Because of the nature of RP-HPLC employed in the separation of intact and modified forms of rCMTI-V and its mutants, the retention time of a given inhibitor is controlled, in part, by its hydrophobicity (Mont & Hodges, 1989; Krause et al., 1995); a mutant that is eluted later than rCMTI-V is expected to be more hydrophobic. Figure 3 presents the RP-HPLC elution profile of rCMTI-V and the five mutants. As anticipated, substitution of either Arg[50] or Arg[52] by the hydrophobic Ala leads to an increase in the retention time; similarly, substitution by the hydrophilic Lys leads to a shorter retention time, in comparison with those of the Arg→Ala mutants. However, in reference to rCMTI-V, the Arg→Lys substitution results in a longer retention time for the two mutants, suggesting that the mutants are more

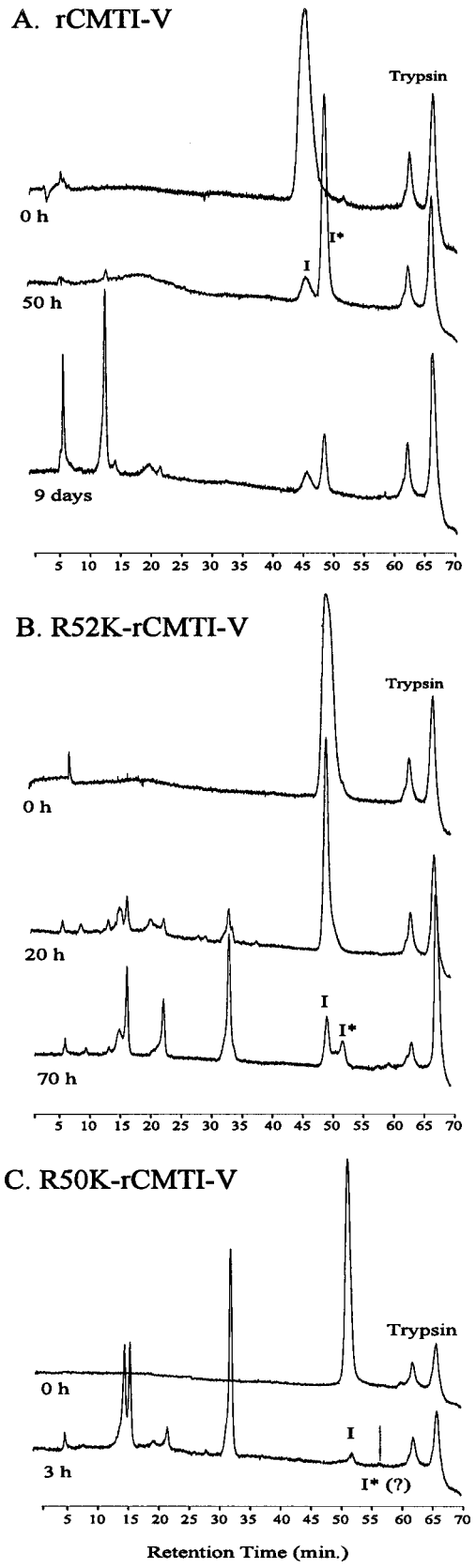

FIGURE 2: RP-HPLC peaks of a mixture of rCMTI-V or a mutant and trypsin (5 mole%) in 50 mM potassium phosphate buffer, pH 6.75, at room temperature (23 °C) at different time intervals. Absorbance was monitored at 280 nm, and, therefore, fragments lacking any aromatic residues were not detected. In the case of the R50 mutants, samples were incubated with 2 mole% trypsin.

hydrophobic. Similarly, the R50Q mutant exhibits a longer retention time than does rCMTI-V, as expected; however,

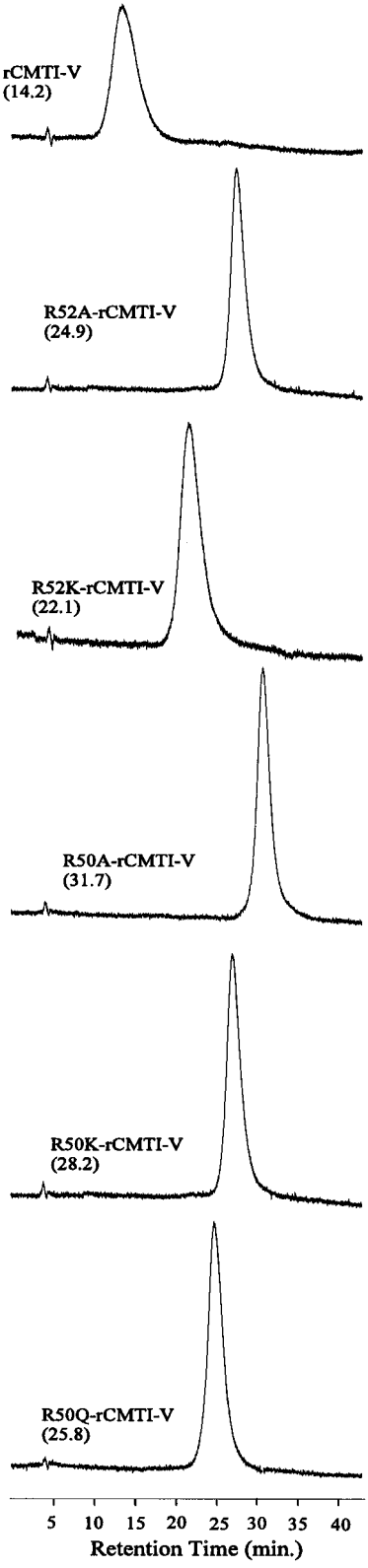

FIGURE 3: Comparison of RP-HPLC retention times of rCMTI-V and the R50 and R52 mutants. The same eluting buffer was used for all the samples under the same experimental conditions at room temperature (23 °C). The numbers within parentheses represent retention times in min.

that mutation results in a reduced retention time as compared to the R50K change.

An interesting observation emerges when the retention times are compared for the mutants R50A and R52A on the one hand and R50K and R52K on the other. In both cases, for the same amino acid composition, mutation at position

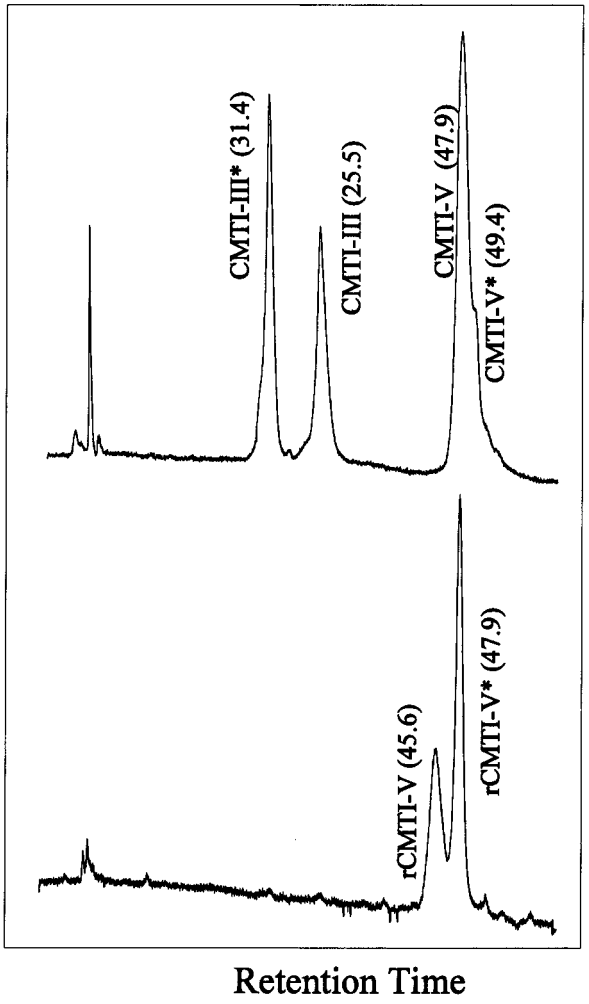

FIGURE 4: RP-HPLC retention time comparison among intact and hydrolyzed forms of CMTI-III, CMTI-V, and rCMTI-V. The same eluting buffer was used under the same experimental conditions. The numbers within parentheses represent retention times in min.

50 has an enhanced effect: the Arg→Ala mutation leads to a net increase of 6.8 min in retention time; similarly, the Arg→Lys substitution results in a net increase of 6.1 min. Clearly, factors other than hydrophobicity also contribute to the observed retention time, and these should be different for the two mutants.

Insight into additional factors that influence the RP-HPLC elution profile is obtained by making use of the conclusion from trypsin hydrolysis studies (Figure 2): Both R50A and R50K are more susceptible to degradation than the corresponding R52 mutants, suggesting that the binding loop in each of the R50 mutants is probably more flexible. Support for this notion is obtained from a comparative RP-HPLC elution profiles of intact and reactive-site hydrolyzed forms of CMTI-III, CMTI-V, and rCMTI-V (Figure 4). In the case of CMTI-III, the hydrolyzed inhibitor elutes earlier, as would be expected because of the formation of a second positively charged amino terminus at the clipped site. This is also true of rCMTI-V, which, unlike CMTI-V, possesses a free amino terminus and hence elutes earlier than the native protein. For CMTI-III, the following thermodynamic quantities were determined (Krishnamoorthi et al., 1992): $K_{hyd} = 2.7$ at 30 °C; $\Delta S° = -9$ eu. The loss in entropy of the system, comprising the protein and water, could be attributed to the ordering of water molecules and/or reduced flexibility of the inhibitor. In the case of ionization of simple organic acids

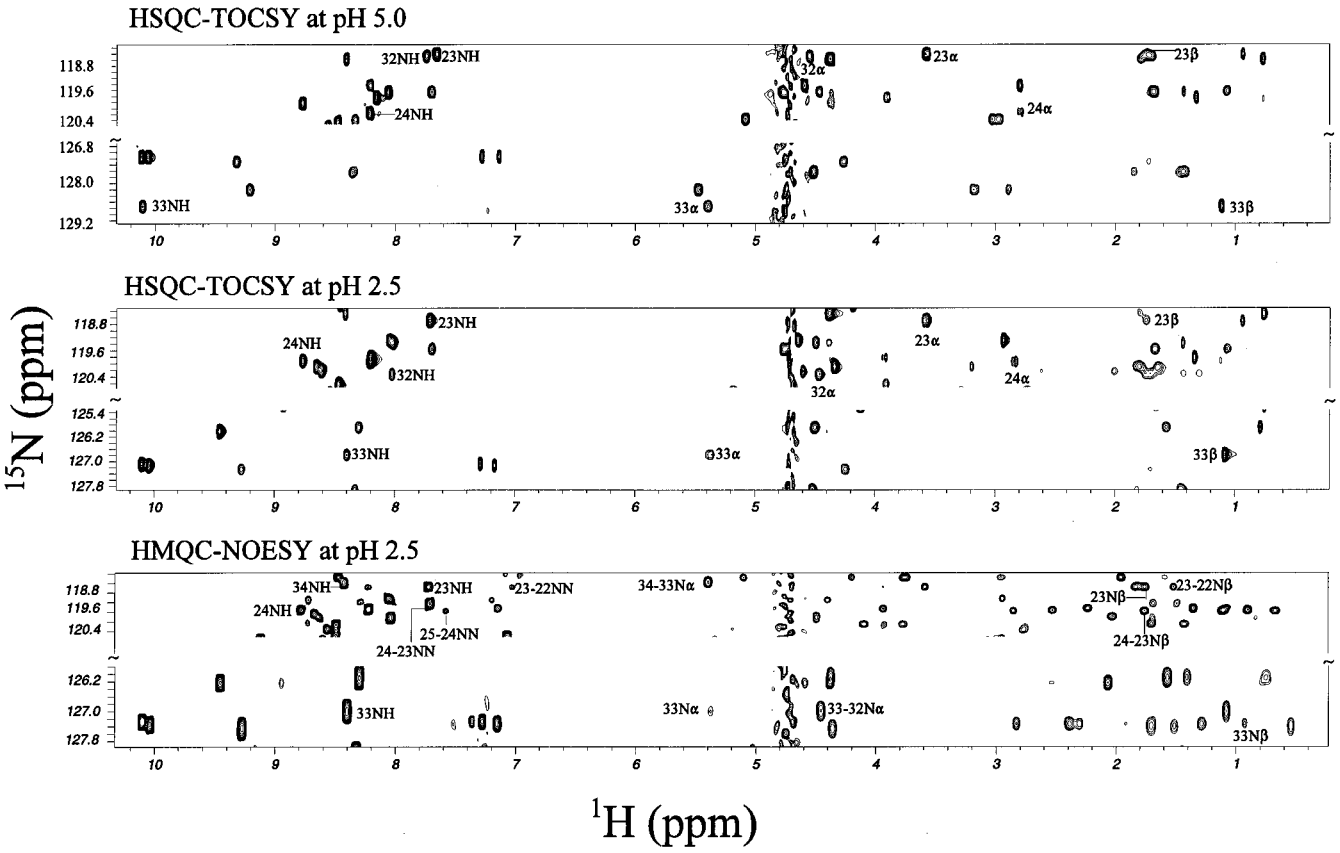

FIGURE 5: Portions of ^{15}N−^{1}H HSQC-TOCSY maps of 70 ms mixing time of rCMTI-V at pH 5.0 and 2.5, showing significant chemical shift differences for Ile[24] and Ala[33] cross-peaks; the unchanged NOE patterns for Ala[33] in a β-strand and Ile[24] in the only α-helical segment are shown in the HMQC-NOESY map at pH 2.5. The notation, such as 24NH, represents the HMQC cross-peak; such as 33Nα, intraresidue NOE between the amide hydrogen and the α-hydrogen; and such as 33-32Nα, sequential NOE from the amide hydrogen of residue, *i*, to the α-hydrogen of residue, *i*−*1*.

in water—a dissociation reaction—the accompanying reduction in entropy was attributed to the ordering of water molecules (March, 1977). In the case of CMTI-V or rCMTI-V, the hydrolyzed form elutes later than the intact form, in spite of the formation of a new positively charged amino terminus, which is hydrophilic. The thermodynamic quantities determined shed light on the factor responsible for this unexpected elution behavior: $K_{hyd} \approx 9$ and $\Delta S° \approx +10$ eu for CMTI-V at 25 °C (Cai et al., 1995b). For rCMTI-V, the respective values are 7 and +11 eu. The positive sign of $\Delta S°$ suggests the increased flexibility of the cleaved binding loop, as evident from the solution structure of CMTI-V* (Cai et al., 1995b). It is noteworthy that $\Delta H°$ is negative for the CMTI-III ⇄ CMTI-III* system (Krishnamoorthi et al., 1992), whereas it is positive for the native or recombinant CMTI-V ⇄ CMTI-V* system. In light of the recent work by Grunwald and Steel (1995) on enthalpy−entropy compensation accompanying solvent reorganization, it may be inferred that solvent interaction with a given inhibitor probably changes between the intact and hydrolyzed forms. In the case of CMTI-V* or rCMTI-V*, the newly formed termini enhance the hydrophobic interaction of the protein with the C-18 column, most likely because of their flexibility. Applying this guideline to the elution behavior of the mutant pairs, R50A and R52A and R50K and R52K, we may infer that in the case of the R50 mutants, the binding loop is more flexible. Conversely, this would mean that the Arg[50] side chain contributes more to the stability and conformation of the binding loop in CMTI-V. Additional insight into the differential stabilizing roles played by Arg[50] and Arg[52] has been obtained from their side-chain dynamics, as determined by NMR spectroscopy.

^{1}H and ^{15}N Resonance Assignments. From a collective consideration of the NOESY, TOCSY, and ^{15}N-edited HSQC-TOCSY and HMQC-NOESY data sets of rCMTI-V at pH 5.0 and 2.5, sequential assignments were made for the protein's backbone atoms (^{1}H and ^{15}N), including main- and side-chain ^{15}N−^{1}H units and most of the side-chain β-hydrogens (Table S-1; supporting information), following standard 2D NMR strategies (Würthrich, 1986). The NMR assignment procedures developed earlier for native CMTI-V (Cai et al., 1995a) and the recombinant protein (Liu et al., 1996) were implemented, which made the current assignment task much easier and more simplified. The ^{1}H and ^{15}N chemical shifts of rCMTI-V at pH 5.0 were found to be the same as those obtained earlier for rCMTI-V at pH 5.4 (Liu et al., 1996). Figure 5 compares a portion of the HSQC-TOCSY map of rCMTI-V at pH 5.0 and 2.5. Also shown is a portion of the HMQC-NOESY map of rCMTI-V at pH 2.5. A combined analysis of the three maps reveals that through-space connectivities are retained even for those residues that exhibit significant chemical shift differences. Thus, it is seen that although the ^{15}N−^{1}H units of Ala[33] and Ile[24] exhibit the largest chemical shift differences due to the pH change, the strong NH−C_αH NOE from Val[34] to Ala[33] and from Ala[33] to Lys[32] are consistent with an unchanged β-strand; similarly, the NH−NH and NH−C_βH connectivities of residues 22−25 indicate that the α-helical structure of rCMTI-V remains unchanged.

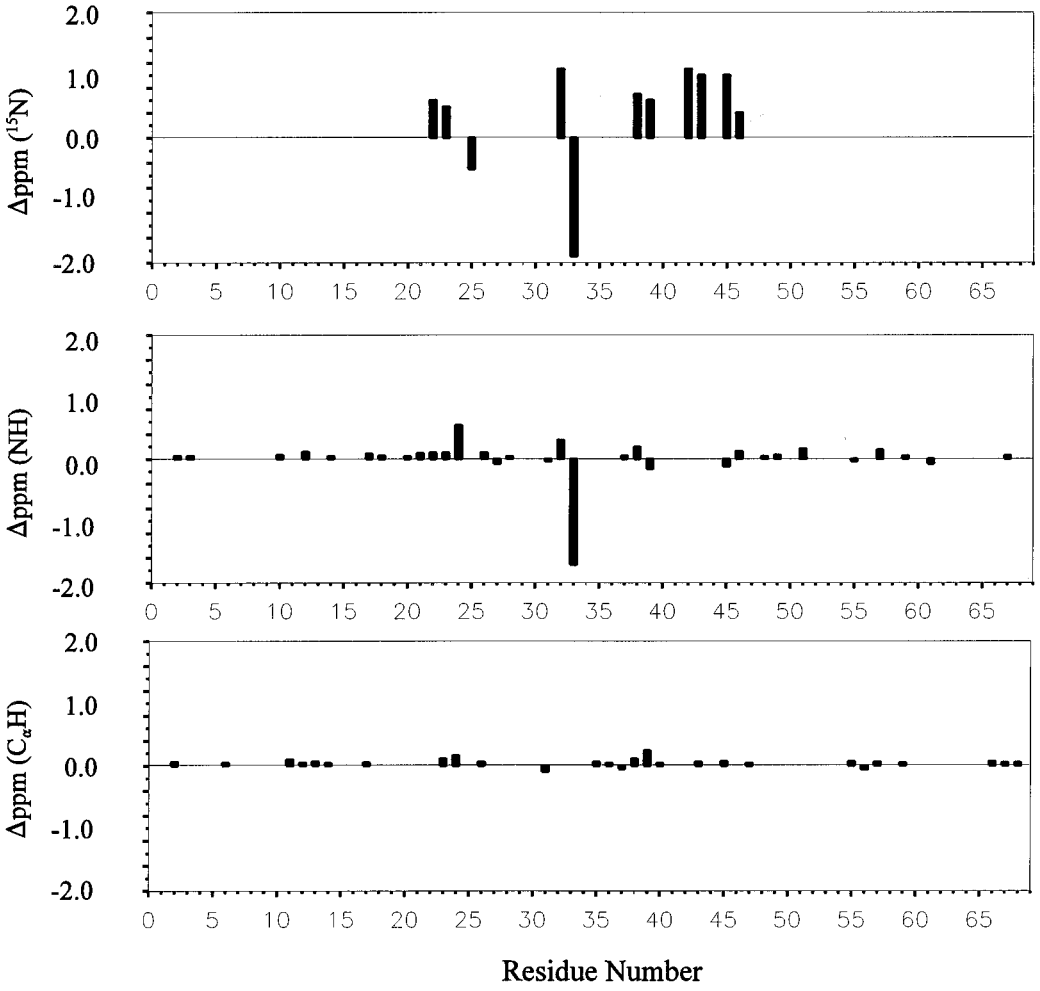

FIGURE 6: ^{15}N and ^{1}H chemical shift differences of backbone atoms of rCMTI-V between pH 2.5 and 5.0 (Δ_{ppm} = $shift_{pH2.5}$ − $shift_{pH5.0}$) as a function of residue number. For the purpose of clarity, values equal to or greater than the error limit of ±0.03 ppm for ^{1}H and ±0.3 ppm for ^{15}N atoms alone are shown.

A comparison of backbone ^{1}H and ^{15}N chemical shifts of rCMTI-V at pH 5.0 and 2.5 is shown in Figure 6. ^{1}H chemical shift differences larger than the error limit of ±0.03 ppm are shown. While many exhibit shift changes less than 0.1 ppm, only three residues exhibit larger NH chemical shift changes: Ala[33] (1.71 ppm), Ile[24] (0.54 ppm), and Lys[32] (0.30 ppm). Similarly, only two residues, Glu[38] and Gly[39], show C_αH chemical shift differences slightly greater than 0.3 ppm; all others show differences smaller than 0.1 ppm. Changes in the ^{15}N chemical shifts (>±0.3 ppm) are noted for residues 22, 23, 25, 32, 33, 38, 39, 42, 43, 45, and 46. The ^{1}H and ^{15}N chemical shifts of arginine side chains and tryptophan side chains are not affected by the pH change (Table S-1; supporting information).

The main-chain ^{15}N chemical shift changes of residues 22, 23, and 25 are attributable to the protonation of Glu[25] at pH 2.5; those of residues 38 and 39 are attributable to the protonation of Glu[37] and Glu[38]; and perturbation of residues 42, 43, 45, and 46 is credited with the protonation of Asp[45]. Thus, many of the observed chemical shift changes may be rationalized as due to neutralization of carboxylate groups (Figure 1).

The ^{1}H chemical shift change of −1.71 ppm observed for the N*H* of Ala[33] provides useful structural information: The side chain of Glu[25] has been found to be rigid, and hence hydrogen-bonded, on the basis of the stereospecific assignments of its β-hydrogens in both CMTI-V (Cai et al., 1995a) and rCMTI-V (Liu et al., 1996). The refined average solution structure of rCMTI-V (Figure 1; Liu et al., 1996) reveals that one of the carboxylate oxygens of Glu[25] lies within 4 Å from the nitrogen of Ala[33] and the side-chain nitrogen of Lys[21]. However, when the pH is lowered from 5.0 to 2.5, the backbone N*H*s of Ala[33] and Lys[32] undergo shift changes of −1.71 and 0.30 ppm, respectively. In contrast, the chemical shift of the backbone N*H* or any of the methylene hydrogens of Lys[21] remains unchanged. These observations point out Ala[33] as the hydrogen-bond partner of Glu[25]. The ^{1}H chemical shift change of Ile[24] may also be attributed to the collapse of the Glu[25]-Ala[33] hydrogen bond at pH 2.5.

Overall, on the basis of a comparison of 2D NMR maps and ^{1}H and ^{15}N chemical shifts, it seems reasonable to conclude that despite some tertiary structural changes, the overall folding of rCMTI-V is not significantly affected by the change in pH. This conclusion is strengthened by the backbone dynamics study, as described below.

Relaxation Measurements of ^{15}N−^{1}H Units in rCMTI-V at pH 5.0 and 2.5. ^{15}N NMR relaxation parameters were measured for 70 NH groups in rCMTI-V at pH 5.0 (Table S-2A; supporting information) that included 62 main-chain units and eight side-chain units from six arginines ($^{15}N_\epsilon$−^{1}Hs) and two from tryptophans ($^{15}N_\epsilon$−^{1}Hs). The pH 2.5 data contained measurements for 69 NH groups (Table S-2B; supporting information); data for Val[61] could not be obtained

Table 1: ^{15}N NMR Relaxation Parameters of Arginine and Tryptophan Side-Chain NH Groups in rCMTI-V at 30 °C

	pH 5.0			pH 2.5		
residue	T_1 (s)	T_2 (s)	NOE	T_1 (s)	T_2 (s)	NOE
R26	0.84 ± 0.10	0.34 ± 0.03	−2.78 ± 0.39	1.68 ± 0.31	0.33 ± 0.03	−1.67 ± 0.31
R47	0.76 ± 0.04	0.30 ± 0.03	−1.29 ± 0.39	1.35 ± 0.81	0.24 ± 0.02	−2.10 ± 0.18
R50	0.45 ± 0.01	0.23 ± 0.02	0.61 ± 0.01	0.46 ± 0.05	0.24 ± 0.01	0.65 ± 0.04
R52	0.52 ± 0.01	0.26 ± 0.01	0.50 ± 0.01	0.52 ± 0.02	0.26 ± 0.02	0.45 ± 0.04
R58	0.86 ± 0.13	0.25 ± 0.03	−2.88 ± 0.36	2.52 ± 0.88	0.29 ± 0.04	−1.00 ± 0.18
R66	0.83 ± 0.11	0.28 ± 0.06	−3.32 ± 0.29	1.11 ± 0.36	0.33 ± 0.05	−1.94 ± 0.18
W9	0.43 ± 0.01	0.19 ± 0.01	0.65 ± 0.02	0.43 ± 0.01	0.17 ± 0.01	0.65 ± 0.04
W54	0.46 ± 0.01	0.19 ± 0.01	0.69 ± 0.01	0.46 ± 0.01	0.16 ± 0.01	0.71 ± 0.04

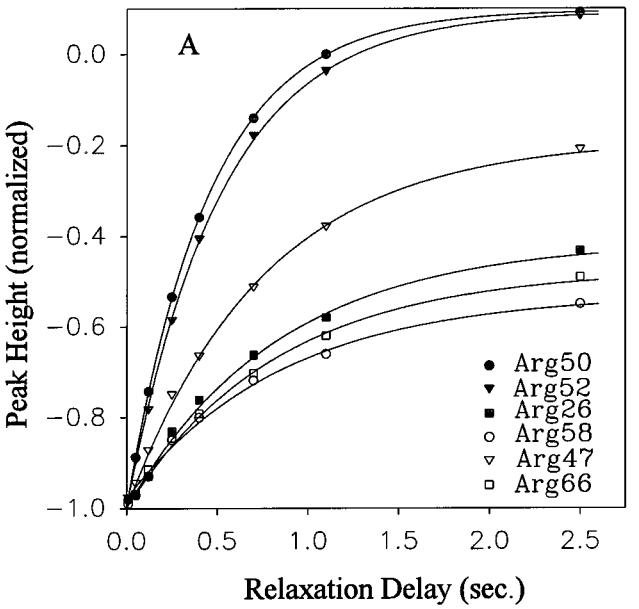

FIGURE 7: Single-exponential least-squares curve fitting of (A) ^{15}N longitudinal relaxation rate (R_1) data and (B) ^{15}N transverse relaxation rate (R_2) data for the arginine N$_\epsilon$Hs in rCMTI-V at pH 5.0. The peak heights are normalized. The computed R_2 curves of Arg[58] and Arg[66] are similar to those of Arg[26] and Arg[47], respectively, and are not shown for the sake of clarity.

due to overlap of its cross-peak with that of one of the lysine side-chain NH_3^+ groups. ^{15}N longitudinal (T_1) and transverse (T_2) relaxation data obtained for the side-chain NH units (N$_\epsilon$Hs) of the six arginines in the protein molecule (Arg[26], Arg[47], Arg[50], Arg[52], Arg[58], and Arg[66]) are depicted in Figure 7A and B, respectively. Better fits were obtained for the main-chain NH groups.

A comparison of the main-chain data sets obtained at pH 5.0 and 2.5 is shown in Figure 8. From the pH 5.0 data sets, an average R_2/R_1 ratio of 2.39 ± 0.20 was computed from 57 main-chain NHs (residues 1−3, 28, and 45 were precluded because their values were lower than the average by more than 1 SD), and the overall tumbling time, τ_m, was optimized at 4.40 ± 0.02 ns, in excellent agreement with the value of 4.43 ± 0.02 ns reported earlier for rCMTI-V at pH 5.4 (Liu et al., 1996). From the pH 2.5 data sets, an average R_2/R_1 ratio of 2.28 ± 0.24 was obtained, which led to an optimized τ_m of 3.97 ± 0.02 ns. The lower value observed at pH 2.5 most likely reflects a change in the hydration of the inhibitor molecule, as negatively charged groups are neutralized. CMTI-V has five negatively charged groups at neutral pH: Glu[25], Glu[37], Glu[38], Asp[45], and the C-terminus. At pH 2.5, all these groups would be protonated and thus neutralized, causing changes in protein hydration. Effects of hydration on protein structure, stability, and dynamics, including internal motions, have been studied both experimentally and by computer simulation (Frauenfelder & Gratton, 1986; Brooks & Karplus, 1986; Kang et al., 1987). The computed general order parameters, S^2, internal correlation times, τ_e, and the exchange terms, Δ_{ex}, for rCMTI-V at pH 5.0 and 2.5 (Tables S-3A and S-3B; supporting information) are compared in Figure 9. The S^2 values are, as expected on the basis of our earlier work (Liu et al., 1996), high for most of the main-chain NH groups; those at the N-terminal and the binding loop exhibit lower values, consistent with increased flexibility. More importantly, the fact that the S^2 values do not change for rCMTI-V at the two different pHs lends support to the conclusion that the overall folding and structure of the inhibitor does not change significantly when the pH is lowered from 5.0 to 2.5. For most of the residues, small values of τ_e (<60 ps) and Δ_{ex} (<0.5 s^{-1}) are obtained. Gly[16] and Gly[17], as noted earlier (Liu et al., 1996), exhibit relatively high values of the exchange term, consistent with their conformational flexibility (Cai et al., 1995a).

^{15}N NMR relaxation parameters (R_1, R_2, and NOE) measured for the N$_\epsilon$H units of Arg[26], Arg[47], Arg[50], Arg[52], Arg[58], Arg[66], Trp[9], and Trp[54] at pH 5.0 and 2.5 are given in Table 1; the model-free parameters computed are given in Table 2. Among the arginines, Arg[50] and Arg[52] have been characterized to be rigid, and the others flexible, on the basis of solution NR studies of CMTI-V (Cai et al., 1995a,c,d) and rCMTI-V at pH 5.4 (Liu et al., 1996). The calculated S^2 values for the arginine residues at pH 5.0 (Table 2) are

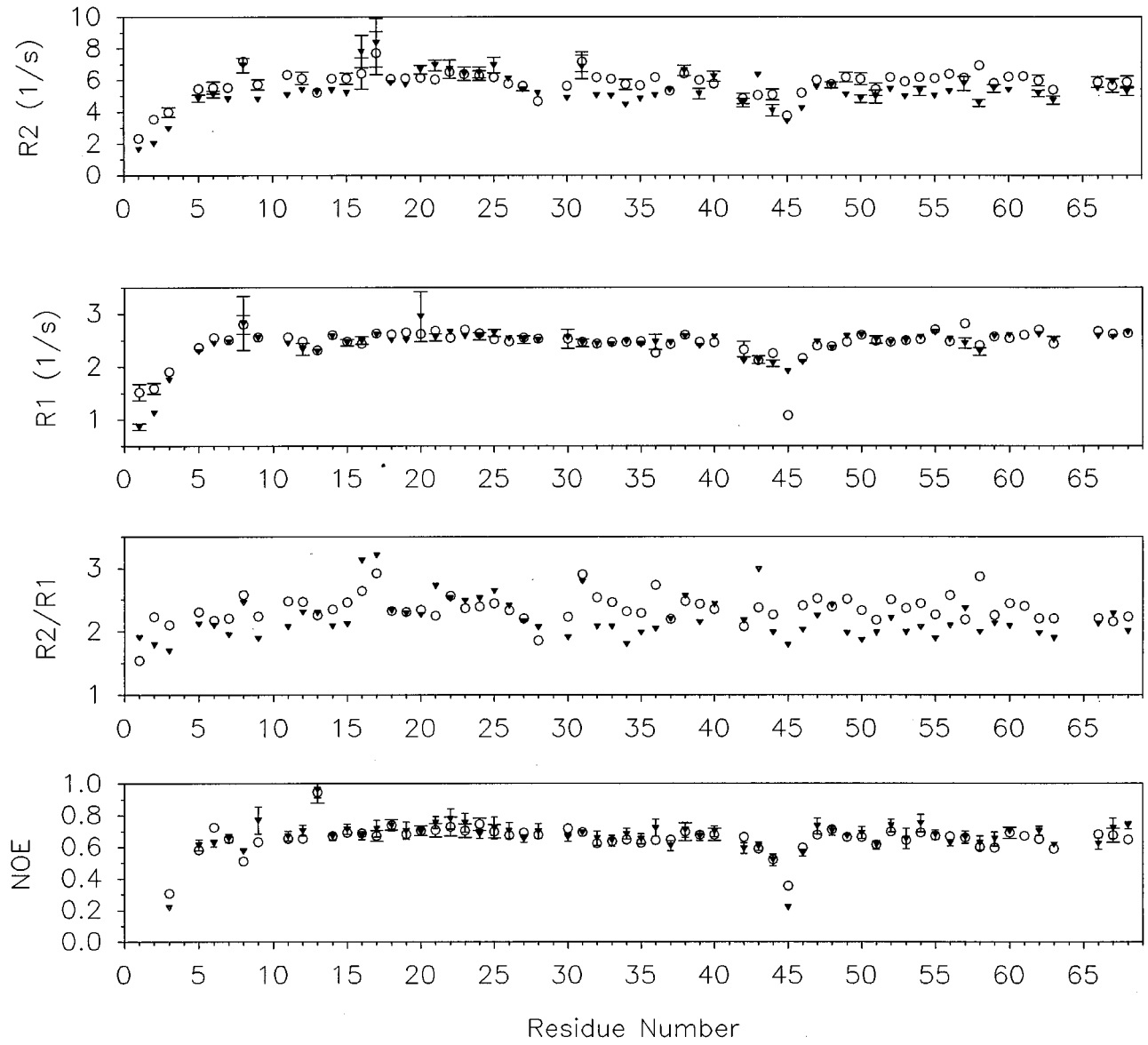

FIGURE 8: Comparison of experimental ^{15}N NMR relaxation parameters (R_1, R_2, R_2/R_1, and NOE values) obtained for the backbone NH groups of rCMTI-V at pH 5.0 (○) and pH 2.5 (▼). Fitting errors are indicated by vertical bars.

Table 2: Model-Free Parameters of Arginine and Tryptophan Side-Chain NHs in rCMTI-V at 30 °C

	pH 5.0			pH 2.5		
residue	S^2	τ_e (ps)	Δ_{ex} (S_{-1})	S^2	τ_e (ps)	Δ_{ex} (S_{-1})
R26	0.03 ± 0.04	321 ± 141	1.70 ± 0.31	0.09 ± 0.02	69 ± 14	2.16 ± 0.36
R47	0.07 ± 0.09	368. ± 262	1.12 ± 0.51	0.05 ± 0.02	52 ± 22	3.63 ± 0.41
R50	0.73 ± 0.01	43 ± 7	0.17 ± 0.26	0.71 ± 0.01	23 ± 11	0.08 ± 0.13
R52	0.63 ± 0.01	53 ± 5	0.04 ± 0.06	0.56 ± 0.02	47 ± 7	0.12 ± 0.17
R58	0.06 ± 0.06	465 ± 141	2.88 ± 0.29	0.18 ± 0.06	126 ± 153	1.84 ± 0.70
R66	0.03 ± 0.03	351 ± 116	2.62 ± 0.81	0.10 ± 0.03	155 ± 97	1.70 ± 0.60
W9	0.79 ± 0.01	38 ± 7	0.02 ± 0.03	0.76 ± 0.01	28 ± 15	0.04 ± 0.05
W54	0.73 ± 0.01	17 ± 5	0.04 ± 0.06	0.72 ± 0.01	6 ± 7	0.01 ± 0.04

consistent with the above conclusion. Buck et al. (1995) have determined S^2 values in the range 0.05−0.30 for mobile arginines in lysozyme. Between Arg^{50} and Arg^{52} in CMTI-V, the former appears to be more rigid. The model-free parameters computed from the pH 2.5 data set reveal that the hydrogen-bonding interactions of Arg^{50} and Arg^{52} with the binding loop persist even at that pH value, at which all carboxylate groups are expected to be protonated. The greater strength and stability of the hydrogen bond involving Arg^{50} is indicated by the significant difference (0.15) between the computed S^2 values for the two residues at pH 2.5. These results strongly suggest that the hydrogen-bonding partners of the two arginines are not carboxylate oxygen atoms.

From the refined average solution structure of rCMTI-V (Figure 1; Liu et al., 1996), it is found that the distances from the side-chain nitrogens of Arg^{52} to the oxygen of Val^{42} and the main-chain and side-chain oxygens of Thr^{43} are all within 5 Å; thus, any of these oxygen atoms is a potential hydrogen-bond acceptor. In the case of Arg^{50}, its rigid side-chain conformation could be defined only to the χ^1 torsion

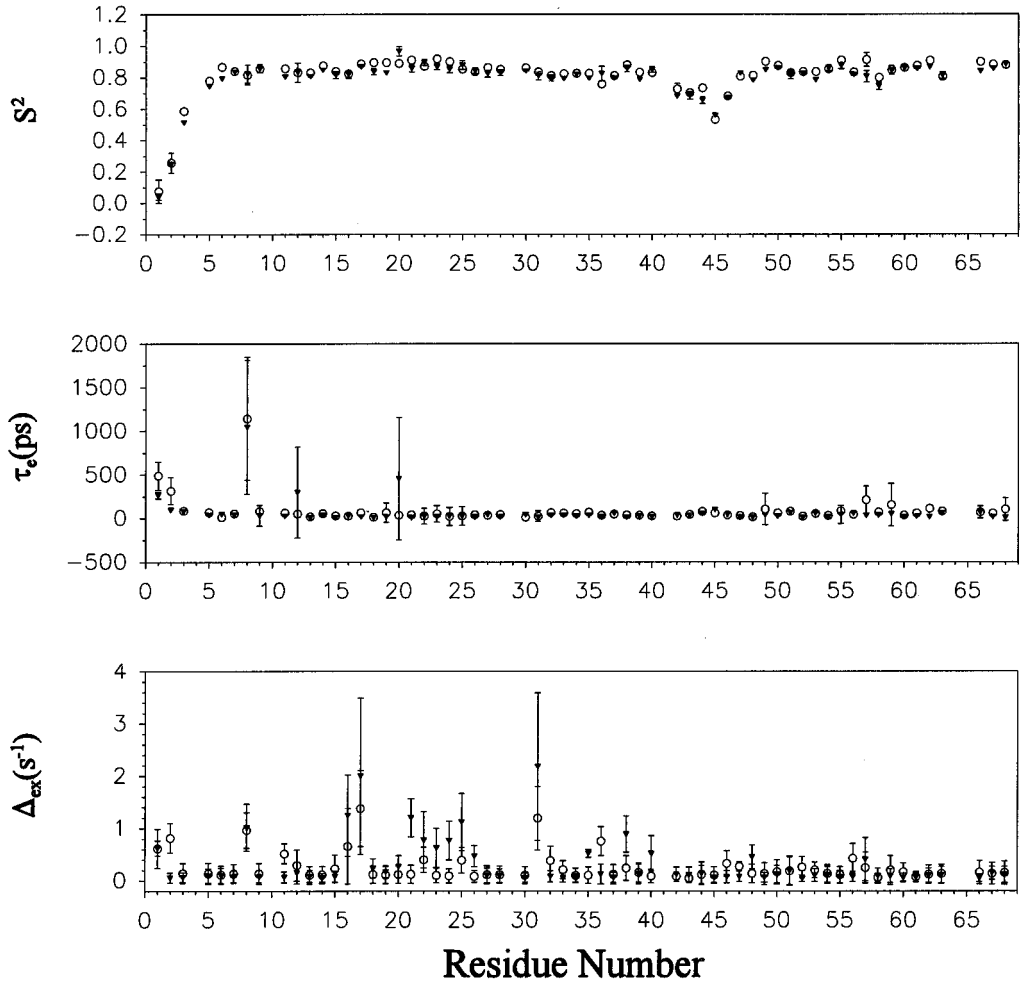

FIGURE 9: Comparison of model-free parameters (S^2, τ_e, and Δ_{ex}) obtained at pH 5.0 (○) and at pH 2.5 (▼) for the backbone NHs in rCMTI-V. Fitting errors are indicated by the vertical bars.

angle because of the chemical shift degeneracy of its δ-hydrogens (Cai et al., 1995a,b). The results of the present study on side-chain dynamics appear to rule out the previously proposed hydrogen bond between the side-chains of Asp[45] and Arg[50] (Cai et al., 1995a). Model-building efforts based on free rotation of the side chain of Arg[50] reveal that any of the main-chain oxygen atoms of residues 45−47 is a potential hydrogen-bond acceptor. X-ray crystallographic studies of eglin c, free (Hipler et al., 1992) and complexed with subtilisin Carlsberg (Bode et al., 1986), reveal that the anchoring arginines (Arg[51] and Arg[53]) retain their hydrogen-bonding and electrostatic interactions with the main-chain oxygen atoms of P_1'(Asp[46]) and P_2(Thr[44]) residues but lose their contacts with the side-chain oxygens of these residues in the free form. Overall, the dynamical parameters determined for the side chains of Arg[50] and Arg[52] indicate that Arg[50] probably contributes more to the stability and, hence, the function of the binding loop in CMTI-V. This is consistent with the recent site-directed mutagenesis experiments (Wen et al., unpublished results), which showed that a 20-fold increase in the amount of the R50A mutant, as opposed to a 11-fold increase in the amount of the R52A mutant, relative to the wild-type protein, was required to cause 50% inhibition of factor XIIa activity.

Side-Chain Dynamics of Trp[9] and Typ[54]. The rings of both tryptophans appear to be rigid, based on their S^2 values, 0.79 for Trp[9] and 0.73 for Trp[54] (Table 2), and their rigidity is not affected by the change in pH. This is consistent with the conclusion that the three-dimensional conformation of the inhibitor molecule is conserved at the lower pH. The dynamical properties evaluated here are also consistent with the structural results: the Trp[9] side chain is located in the core of the protein and is stabilized through hydrogen-bonding and hydrophobic interactions with the surrounding groups, as described earlier (Cai et al., 1995a). In the case of Trp[54], a hydrogen bond is indicated between its N_ϵ atom and the main-chain oxygen of Arg[52] as the distance between them is only 3.3 Å (Liu et al., 1996). A large number of hydrophobic interactions between the Trp[54] ring and the binding loop are also indicated: van der Waals contacts within 4 Å: between heavy atoms of the Trp[54] ring and 16 hydrophobic atoms of Leu[36], five of Glu[37], nine of Glu[38], ten of Thr[40], and four of Val[42]. Most likely, these interactions contribute not only to the rigidity of the Trp[54] ring but also to the stability of the binding loop. Apparently, these interactions are preserved at pH 2.5, as the S^2 value is unchanged at the lower pH (Table 2).

CONCLUSIONS

Both Arg[50] and Arg[52] in CMTI-V impart conformational stability to the binding loop by hydrogen-bonding interactions. Removal of these interactions results in increased binding loop flexibility and hence susceptibility to proteolysis. For rCMTI-V and mutants, the RP-HPLC retention time appears to provide a qualitative measure of the relative flexibility of the binding loop. Arg[50] makes a stronger

hydrogen bond than does Arg^{52} and appears to contribute more to binding loop stability. The protein core−binding loop hydrogen bonds made by Arg^{50} and Arg^{52} do not seem to involve carboxylate groups as hydrogen-bond acceptors.

ACKNOWLEDGMENT

We thank Dr. Arthur G. Palmer, III, Columbia University, New York, for providing us a copy of the model-free software used in the study and Mrs. Yuxi Gong and Mr. Dave Manning for their technical assistance.

SUPPORTING INFORMATION AVAILABLE

One figure showing the temperature dependence of $\Delta G°$ for rCMTI-V ⇌ rCMTI-V* and five tables containing ^1H and ^{15}N assignments of rCMTI-V at pH 2.5, experimental R_1, R_2, and NOE measurements at pH 5.0 and 2.5, and model-free parameters (S^2, τ_e, and Δ_{ex}) at both pHs (17 pages). Ordering information is given on any current masthead page.

REFERENCES

Anil Kumar, Ernst, R. R., & Wüthrich, K. (1980) *Biochem. Biophys. Res. Commun. 95*, 1−6.
Ardelt, W., & Laskowski, M., Jr. (1991) *J. Mol. Biol. 220*, 1041−1053.
Bax, A., & Davis, D. G. (1985) *J. Magn. Reson. 65*, 355−360.
Bax, A., Griffey, R. H., & Hawkins, B. L. (1983) *J. Magn. Reson. 55*, 301−315.
Bode, W., Papmokos, E., Musil, D., Seemuller, U., & Fritz, H. (1986) *EMBO J. 5*, 813−818.
Bodenhausen, G., & Ruben, D. J. (1980) *Chem. Phys. Lett. 69*, 185−189.
Brooks, C. L., & Karplus, M. (1986) *Methods Enzymol. 127*, 369−400.
Buck, M., Boyd, J., Redfield, C., Mackenzie, D. A., Jeenes, D. J., Archer, D. B., & Dobson, C. M. (1995) *Biochemistry 34*, 4041−4055.
Cai, M., Gong, Y., Kao, J. L.-F., & Krishnamoorthi, R. (1995a) *Biochemistry 34*, 5201−5211.
Cai, M., Gong, Y., Prakash, O., & Krishnamoorthi, R. (1995b) *Biochemistry 34*, 12087−12094.
Cai, M., Liu, J., Gong, Y., & Krishnamoorthi, R. (1995c) *J. Magn. Reson., Ser. B 107*, 172−178.
Cai, M., Gong, Y., & Krishnamoorthi, R. (1995d) *J. Magn. Reson., Ser. B 106*, 297−299.
Cai, M., Huang, Y.; Prakash, O., Wen, L., Han, S. K., & Krishnamoorthi, R. (1995e) *J. Magn. Reson., Ser. B 108*, 189−191.
Cavanagh, J., Palmer, A. G., Wright, P. E., & Rance, M. (1991) *J. Magn. Reson. 91*, 429−436.
Clore, G. M., Gronenborn, A. M., Kjaer, M., & Poulsen, F. M. (1987a) *Protein Eng. 1*, 305−311.
Clore, G. M., Gronenborn, A. M., James, M. N. G., Kjaer, M., McPhalen, C. A., & Poulsen, F. M. (1987b) *Protein Eng. 1*, 313−318.
Clore, G. M., Driscoll, P. C., Wingfield, P. T., & Gronenborn, A. M. (1990) *Biochemistry 29*, 7387−7401.
Frauenfelder, H., & Gratton, E. (1986) *Methods Enzymol. 127*, 207−216.
Grunwald, E., & Steel, C. (1995) *J. Phys. Chem. 117*, 5687−5692.
Hipler, K., Priestle, J. P., Rahuel, J., & Grutter, M. G. (1992) *FEBS Lett. 309*, 139−145.
Hyberts, S. G., Goldberg, M. S., Havel, T. F., & Wagner, G. (1992) *Protein Sci. 1*, 736−751.
Kang, Y. K., Nemethy, G., & Scheraga, H. A. (1987) *J. Phys. Chem. 91*, 4105−4109.
Kördel, J., Skelton, H. J., Akke, M., Palmer, A. G., & Chazin, W. J. (1992) *Biochemistry 31*, 4856−4866.
Krause, E., Beyermann, M., Dathe, M., Rothemund, S., & Bienert, M. (1995) *Anal. Chem. 67*, 252−258.
Krishnamoorthi, R., Gong, Y., & Richardson, M. (1990) *FEBS Lett. 273*, 163−167.
Krishnamoorthi, R., Lin, C. S., & VanderVelde, D. (1992) *Biochemistry 31*, 4965−4969.
Lashowski, M., Jr., & Kato, I. (1980) *Annu. Rev. Biochem., 49*, 593−626.
Lipari, G., & Szabo, A. (1982a) *J. Am. Chem. Soc., 104*, 4546−4559.
Lipari, G., & Szabo, A. (1982b) *J. Am. Chem. Soc., 104*, 4559−4570.
Liu, J., Prakash, O., Cai, M., Gong, Y., Huang, Y., Wen, L., Wen, J. J., Huang, J.-K., & Krishnamoorthi, R. (1996) *Biochemistry 35*, 1516−1524.
Live, D. H., Davis, D. G., Agosta, W. C., & Cowburn, D. (1984) *J. Am. Chem. Soc. 106*, 1939−1941.
Mant, C. T., & Hodges, R. S. (1989) *J. Liq. Chromtogr. 12*, 139−172.
March, J. (1977) *Advanced Organic Chemistry*, 2nd ed., pp 244−245, McGraw-Hill, New York.
McPhalen, C. A., & James, M. N. G. (1987) *Biochemistry 26*, 261−269.
Meiboon, S., & Gill, D. (1958) *Rev. Sci. Instrum. 29*, 688−691.
Müller, L. (1979) *J. Am. Chem. Soc. 101*, 4481−4484.
Noggle, J. H., & Shirmer, R. E. (1971) *The Nuclear Overhauser Effect: Chemical Applications*, Academic Press, New York.
Palmer, A. G., Rance, M., & Wright, P. E. (1991) *J. Am. Chem. Soc., 113*, 4370−4380.
Peng, J. W., & Wagner, G. (1994) *Methods Enzymol. 239*, 563−596.
Shaw, G. L., Davis, B., Keeler, J., & Fersht, A. R. (1995) *Biochemistry 34*, 2225−2233.
Skelton, N. J., Palmer, A. G., Akke, M., Kördel, J., Rance, M., & Chazin, W. (1993) *J. Magn. Reson. Ser. B 102*, 253−264.
Stone, M. J., Fairbrother, W. J., Palmer, A. G., III, Reizer, J., Saier, M. H., Jr., & Wright, P. E. (1992) *Biochemistry 31*, 4394−4406.
Vold, R. L., Waugh, J. S., Klein, M. P., & Phelps, D. E. (1968) *J. Chem. Phys. 48*, 3831−3832.
Wen, L., Kim, S.-S., Tinn, T. T., Huang, J.-K., Krishnamoorthi, R., Gong, Y., Lwin, Y. N., & Kyin, S. (1993) *Protein Expression Purif. 4*, 215−222.
Wieczorek, M., Otlewski, J., Cook, J., Parks, M., Leluk, J., Wilimowska-plec, A., Polanowski, A., Wilusz, T., & Laskowski, M., Jr. (1985) *Biochem. Biophys. Res. Commun. 126*, 646−652.
Würthrich, K. (1986) *NMR of Proteins and Nucleic Acids*, Wiley & Sons, New York.

BI953038A